National Conference with International Participation
ENGINEERING MECHANICS 2007
Svratka, Czech Republic, May 14 – 17, 2007

COMPUTATION OF DYNAMIC PROPERTIES OF AEROSTATIC JOURNAL BEARINGS

A. Skarolek*, **J. Kozánek****

Summary: *This contribution deals with computation of stiffness and damping coefficients of aerostatic bearings. Model of bearings is based on Reynolds equation for compressible medium supplemented by description of mass flow through feeding system. Time-series of displacements and internal force are obtained by numerical solution. Linear stiffness and damping coefficients are obtained by means of least squares regression.*

1. Introduction

Externally pressurized gas bearings have some valuable advantages in comparison of oil bearings. These attributes are for instance higher precision, low noise, high durability, lower heat generation and less contamination. The main disadvantage of gas bearings is their possible low stability. The instability of aerostatic bearings has to be avoided during operation, because it mostly means a serious damage to equipment. Some problems of aerostatic bearing stability are shown in works of Czołczyński & Kapitaniak (1997), Czołczyński (1993).

The bearing is commonly represented by sets of stiffness and damping coefficients, which is suitable for computation of stable regions and amplitudes of forced vibrations. Classical approach to obtain these properties is to solve perturbed Reynolds equation. This method has been often used for self-acting gas bearings and even more frequently for oil bearings, but it can be also used in case of externally pressurized gas bearing by introducing air mass flow variations (Han et al., 1994). The other way is to solve Reynolds equation for compressible medium in time domain together with equations of journal motion (Skarolek & Kozánek, 2006). The bearing thereby is treated as more real than in method mentioned above. The results are not limited to case of small displacements and even non-linear coefficients of stiffness and damping is obtainable in sense of internal bearing force to be considered as polynomial function of displacements and velocities (Czołczyński, 1999).

*Ing. Antonín Skarolek: Department of Mechanics and Elasticity, Faculty of Mechanical Engineering, Technical University of Liberec, Hálkova 6, Liberec, 460 01, Czech Republic, e-mail: antonin.skarolek@gmail.com

**Ing. Jan Kozánek, CSc.: Institute of Thermomechanics, Academy of Sciences of the Czech Republic, Dolejškova 5, Prague, 182 00, Czech Republic, e-mail: kozanek@it.cas.cz

The aim of the paper is to determine these dynamic properties of the specific aerostatic bearings. The results will be compared with results obtained from experimental investigation on rotor stand (Šimek et al., 2007), which is already built at FME, CTU, Prague for validation of the methods.

2. Investigated aerostatic bearings

Two different bearing shapes have been considered. The former has one row of feeding orifices situated in the middle of bearing (type A), the latter has two rows of orifices placed in quarters of bearing length (type B). There are eight orifices evenly located on bearing periphery in every row of either types of bearing. Schematics of the bearings are shown on fig.1. Both of the bearing types have been designed by Techlab, Ltd., Prague.

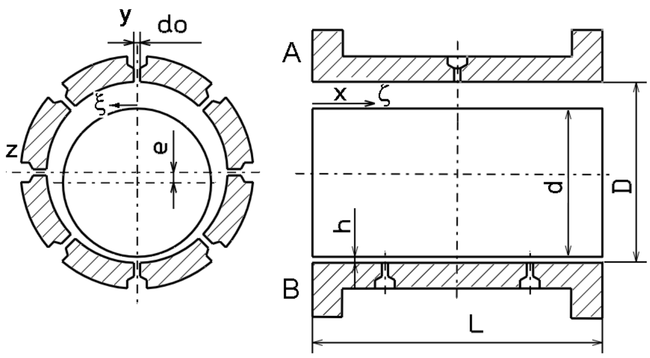

Figure 1: Radial aerostatic bearings

3. Mathematical model of bearing

Equations of motion of shaft journal for two translational lateral degrees of freedom are:

$$m\ddot{y} = F_y - mg + Q_y, \qquad m\ddot{z} = F_z + Q_z. \tag{1}$$

F_y, F_z mean components of internal force of bearing and Q_y, Q_z mean excitation forces acting upon journal. Internal force is determined by pressure distribution in bearing, which is given by Reynolds equation supplemented by terms of air mass flow through feeding system. Dimensionless form of Reynolds equation for compressible medium

$$-\frac{\partial}{\partial\xi}\left[PH^3\frac{\partial P}{\partial\xi}\right]-\frac{\partial}{\partial\zeta}\left[PH^3\frac{\partial P}{\partial\zeta}\right]+\Lambda_\xi\frac{\partial}{\partial\xi}[PH]+\frac{\partial}{\partial\tau}[PH]=C\frac{\mathrm{d}\dot{m}}{\mathrm{d}\xi\mathrm{d}\zeta}, \quad C=\frac{12\mu r T_0}{p_a c^3} \tag{2}$$

is established with dimensionless values

$$P=\frac{p}{p_a}, \quad H=\frac{h}{c}, \quad \zeta=\frac{x}{R}, \quad \Lambda_\xi=\frac{6\mu\omega R^2}{p_a c^2}, \quad \tau=\frac{p_a c^2}{12\mu R^2}t=\frac{\omega}{2\Lambda_\xi}t, \tag{3}$$

by means of atmospheric pressure p_a, radius of bearing R, angular velocity of journal ω, radial clearance c and air viscosity μ. Right-hand side of (2) involves mass flow of supplied air $\dot{m}$, which is nonzero only at areas of feeding orifices. St. Venant - Wantzel's formula is used to determine the air mass flow

$$\dot{m} = C_v A_v p_0 \sqrt{\frac{2\kappa}{\kappa - 1} \frac{1}{rT_0} \left[1 - \beta^{\frac{\kappa-1}{\kappa}}\right]} \beta^{\frac{1}{\kappa}}, \quad \beta = \max\left\{\frac{p}{p_0}, \beta^*\right\}, \quad \beta^* = \left(\frac{2}{\kappa+1}\right)^{\frac{\kappa}{\kappa-1}}. \quad (4)$$

In the equation (4) the symbol A_v means cross section area of feedhole and the symbol C_v means discharge coefficient according to Czołczyński (1999):

$$A_v = \pi r_0^2, \qquad C_v = 0.85 - 0.15\beta - 0.1\beta^2. \quad (5)$$

The internal force of bearing is evaluated from pressure distribution within the air layer as follows

$$F_y = -p_a R^2 \int_0^{2\pi} \int_0^{L/R} P(\xi, \zeta) \cos(\xi) \, d\zeta d\xi,$$
$$F_z = -p_a R^2 \int_0^{2\pi} \int_0^{L/R} P(\xi, \zeta) \sin(\xi) \, d\zeta d\xi. \quad (6)$$

There is more complex mathematical model of aerostatic bearing presented in recent works (Skarolek & Kozánek, 2006; Skarolek, 2007). It respects tilting degrees of freedom of journal and also internal bearing torques. Simplified, hereby established model allows us to obtain only stiffness and damping coefficients related to translational displacements of journal centre.

4. Discretization and numerical methods

The method of finite differences is used for discretization of the Reynolds equation (2). The circumferential coordinate $\xi \in < 0, 2\pi >$ has been divided into m segments, the axial one $\zeta \in < 0, \frac{L}{R} >$ into n segments. Created equidistant mesh with $(m+1) \cdot (n+1)$ nodes divides the air layer into $m \cdot n$ subregions. Two rows and one column of nodes are attached to the mesh in order to implement the boundary and periodic conditions. See figure 2. The

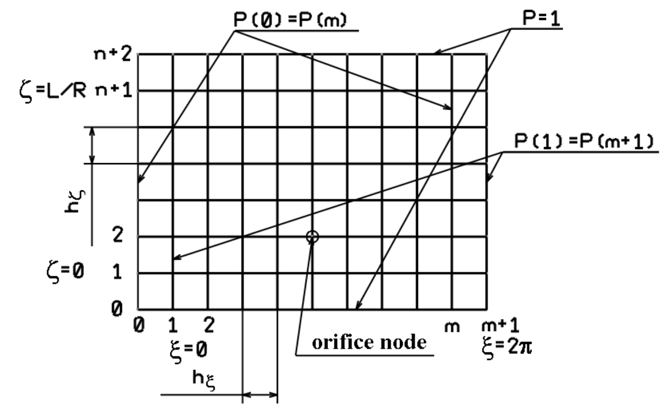

Figure 2: Mesh of the air film area

spatial derivatives have been replaced by finite differences in the equation (2). A system of non-linear differential equations with pressure as dependent variable has arisen

$$\frac{\partial P}{\partial \tau}(i,j) = \frac{1}{H_{i,j}}[P_{i,j}H_{i,j}^3\frac{P_{i+1,j}-2P_{i,j}+P_{i-1,j}}{h_\xi^2} + P_{i,j}H_{i,j}^3\frac{P_{i,j+1}-2P_{i,j}+P_{i,j+1}}{h_\zeta^2} +$$
$$H_{i,j}^3\left(\frac{P_{i+1,j}-P_{i-1,j}}{2h_\xi}\right)^2 + H_{i,j}^3\left(\frac{P_{i,j+1}-P_{i,j-1}}{2h_\zeta}\right)^2 + 3P_{i,j}H_{i,j}^2\frac{\partial H}{\partial \xi}(i,j)\frac{P_{i+1,j}-P_{i-1,j}}{2h_\xi} +$$
$$3P_{i,j}H_{i,j}^2\frac{\partial H}{\partial \zeta}(i,j)\frac{P_{i,j+1}-P_{i,j-1}}{2h_\zeta} - \Lambda_\xi\left(H_{i,j}\frac{P_{i+1,j}-P_{i-1,j}}{2h_\xi} + P_{i,j}\frac{\partial H}{\partial \xi}(i,j)\right) -$$
$$P_{i,j}\frac{\partial H}{\partial \tau}(i,j) + C\frac{C_v A_v p_0}{h_\xi\, h_\zeta}\sqrt{\frac{2\kappa}{\kappa-1}\frac{1}{rT_0}\left[1-\left(\frac{P_{i,j}}{P_0}\right)^{\frac{\kappa-1}{\kappa}}\right]}\left(\frac{P_{i,j}}{P_0}\right)^{\frac{1}{\kappa}}]. \tag{7}$$

It describes time behaviour of the pressure distribution in relation to the thickness function and its rate of change. Thickness function and its time derivative are obtained from actual position and velocity of journal centre.

Dynamic systems (1) and (7) have been solved separately for each time step of numerical method. Actual position and velocity of journal generate the thickness function and its time derivative. Computation of one time step of system (7) follows. Solved pressure distribution gives us the reactions acting on journal from (6). Single time step of journal equations of motion (1) is solved using just calculated reactions, and entire process is repeated for the next time step. There are two main reasons, why the systems are solved separately during single time step. First is to avoid time-consuming calculations of reactions and thickness functions, which could be computed many times in one time step, if some implicit method was used. The second reason is an assurance of method stability, which depends on eigenvalues of Jacobi matrix of system, time step and stable region of used method. Absolute stability of explicit methods are strongly limited, and evaluation of Jacobi matrix eigenvalues would not be effective. Therefore, authors made an compromise between method stability and algorithm efficiency. A-stable Adams–Moulton method of order two is used for solving system (7) and the fourth order Runge–Kutta method is used for solving system (1), similarly to previous works (Skarolek & Kozánek, 2006; Skarolek, 2007).

5. Obtaining dynamic properties

The numerical model governed above is used for enumeration of stiffness and damping coefficients. Presented approach leads to computation of equilibrium position of journal within bearing and then to solving time-series of internal forces and displacements caused by kinematical excitation of journal centre. Finally, stiffness and damping coefficients are estimated by least squares regression.

Linear model of aerostatic bearings predicts the reaction force components

$$\begin{pmatrix} F_y - F_y^e \\ F_z - F_z^e \end{pmatrix} = \begin{bmatrix} k_{yy} & k_{yz} \\ k_{zy} & k_{zz} \end{bmatrix}\begin{pmatrix} y - y^e \\ z - z^e \end{pmatrix} + \begin{bmatrix} b_{yy} & b_{yz} \\ b_{zy} & b_{zz} \end{bmatrix}\begin{pmatrix} \dot{y} \\ \dot{z} \end{pmatrix}, \tag{8}$$

where F_y^e, F_z^e are an internal force components, acting in journal position y^e, z^e of equilibrium. Journal centre is treated to small harmonic displacements in both directions,

$$\tilde{y} = y - y^e = A \cdot sin(\omega\nu t), \qquad \dot{\tilde{y}} = \dot{y} = A\omega\nu \cdot cos(\omega\nu t), \tag{9}$$

and

$$\tilde{z} = z - z^e = A \cdot sin(\omega\nu t), \qquad \dot{\tilde{z}} = \dot{z} = A\omega\nu \cdot cos(\omega\nu t) \tag{10}$$

separately, after the equilibrium y^e, z^e and F_y^e, F_z^e have been obtained by simulation of systems (1), (7). Before using least squares regression on computed time-series of internal forces and displacements, we should divide the equation (8) into four independent equations,

$$F_{yy} = k_{yy} \cdot \tilde{y} + b_{yy} \cdot \dot{\tilde{y}}, \qquad F_{zy} = k_{zy} \cdot \tilde{y} + b_{zy} \cdot \dot{\tilde{y}}, \tag{11}$$

$$F_{yz} = k_{yz} \cdot \tilde{z} + b_{yz} \cdot \dot{\tilde{z}}, \qquad F_{zz} = k_{zz} \cdot \tilde{z} + b_{zz} \cdot \dot{\tilde{z}}. \tag{12}$$

The functions $\tilde{y}$,$\dot{\tilde{y}}$ and $\tilde{z}$,$\dot{\tilde{z}}$ are orthogonal in sense of scalar product, defined on Lebesgue L^2 function space. This is the reason, why authors prefer kinematical actuating against force excitation. Even if the external force was acting in single direction, steady-state motion of journal consists of both displacements, horizontal and vertical, due to dynamic effect of air layer when journal is revolving. Specially the excitation of the journal by force of unbalanced rotating mass, which produces almost circular motion for lesser eccentricities of journal in bearing, seems to be useless for least square regression, because the displacements are not only dependent, but functions $\tilde{y}$ and $\dot{\tilde{z}}$ become closely collinear (and $\tilde{z}$ become closely collinear with $\dot{\tilde{y}}$).

6. Results

Stiffness and damping coefficients versus argument ν has been solved for both bearing types, A and B, for speed of journal $\omega = 1047\,\mathrm{rad\,s^{-1}}$. Radial clearance of bearings was $c = 32.5\,\mu$m for the type A, and $c = 22.5\,\mu$m for the type B. Other parameters were shared for both these types. Bearing length $L = 45\,$mm, journal radius $R = 15\,$mm, diameter of feedholes $d_0 = 0.2\,$mm, journal mass $m = 4\,$kg and supplied air pressure $p_0 = 3\,p_a \doteq 0.3\,$MPa. Figures 3, 4 show computed dynamic coefficients for bearing type A, figures 5, 6 for bearing type B. Relative eccentricity forced by journal mass was $\varepsilon = 0.44$ for bearing A and $\varepsilon = 0.25$ for bearing B.

Considering $\nu = 1$ (vibration due to rotating unbalanced mass), dependency of dynamic properties on journal angular speed has been computed, with other values mentioned above. See fig. 7, 8 for bearing A, fig. 9, 10 for bearing B. Fig. 11, 12 show equilibrium in relation to ω.

Eigenvalues of the system

$$\begin{bmatrix} m & 0 \\ 0 & m \end{bmatrix} \begin{pmatrix} \ddot{\tilde{y}} \\ \ddot{\tilde{z}} \end{pmatrix} + \begin{bmatrix} b_{yy} & b_{yz} \\ b_{zy} & b_{zz} \end{bmatrix} \begin{pmatrix} \dot{\tilde{y}} \\ \dot{\tilde{z}} \end{pmatrix} + \begin{bmatrix} k_{yy} & k_{yz} \\ k_{zy} & k_{zz} \end{bmatrix} \begin{pmatrix} \tilde{y} \\ \tilde{z} \end{pmatrix} = \begin{pmatrix} 0 \\ 0 \end{pmatrix} \tag{13}$$

have been computed using obtained stiffness and damping coefficients, their real and imaginary parts are shown on fig. 13, 14.

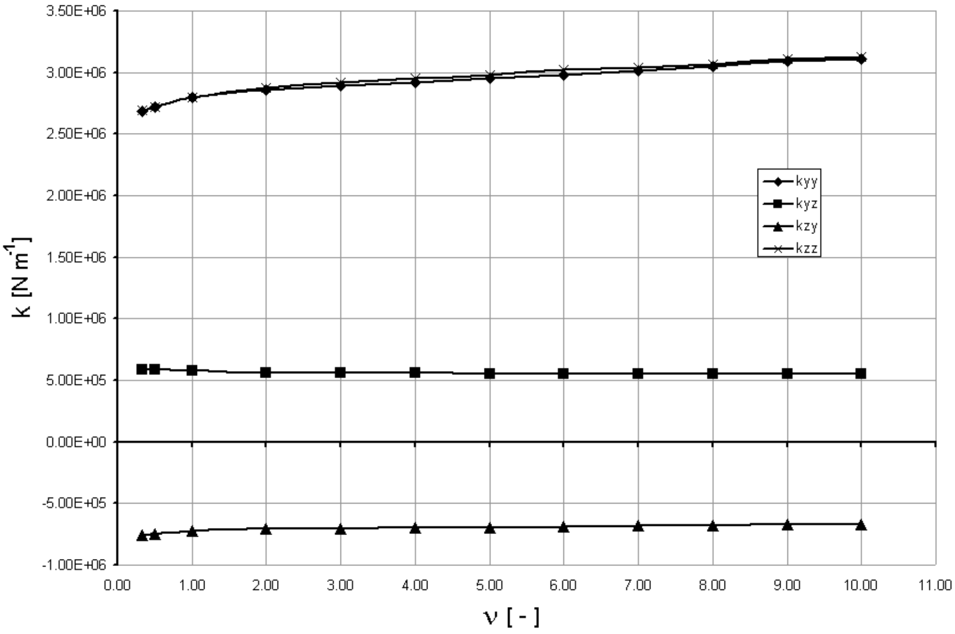

Figure 3: Stiffness vs. ν, Bearing A

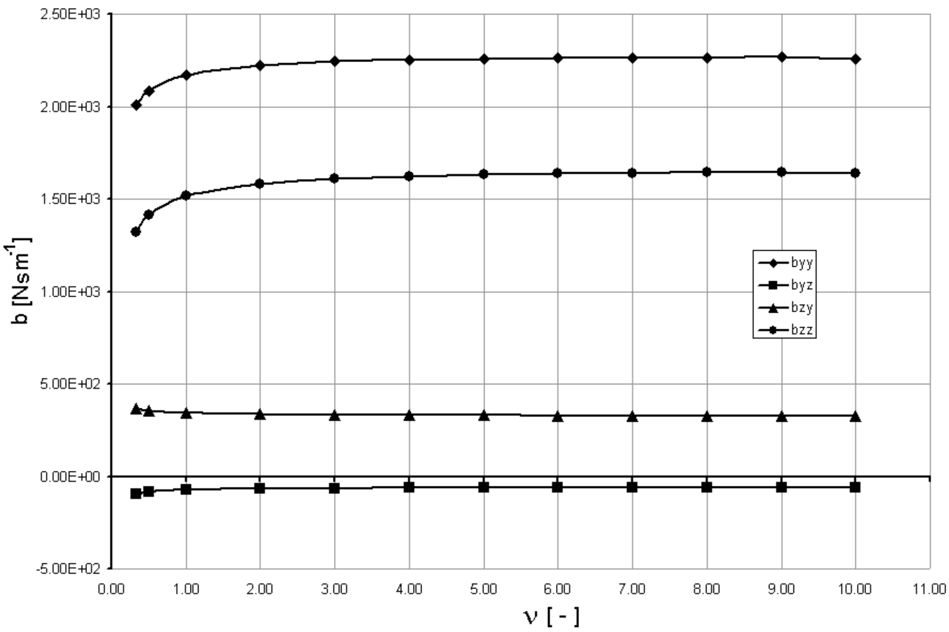

Figure 4: Damping coefficient vs. ν, Bearing A

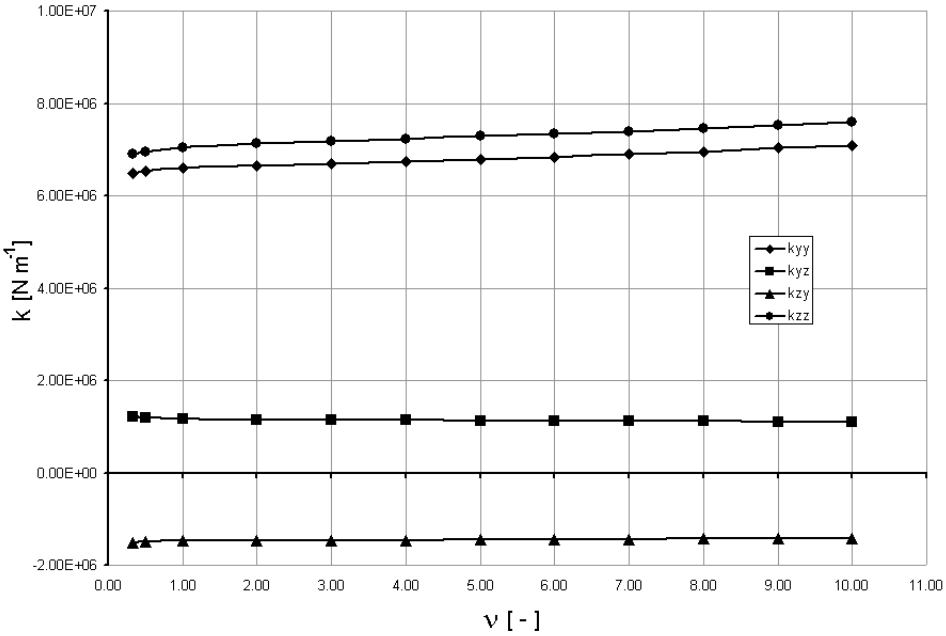

Figure 5: Stiffness vs. ν, Bearing B

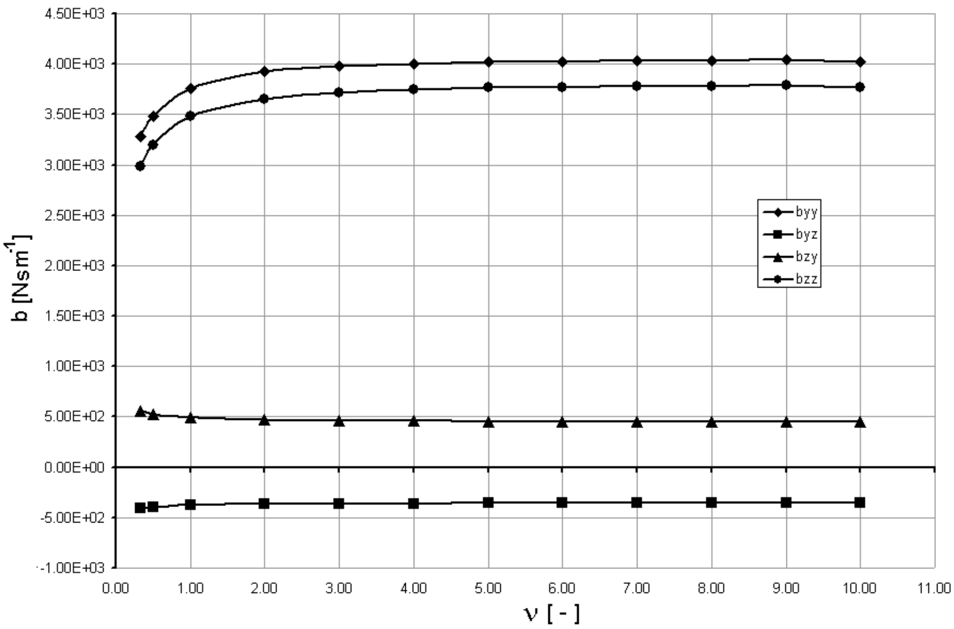

Figure 6: Damping coefficient vs. ν, Bearing B

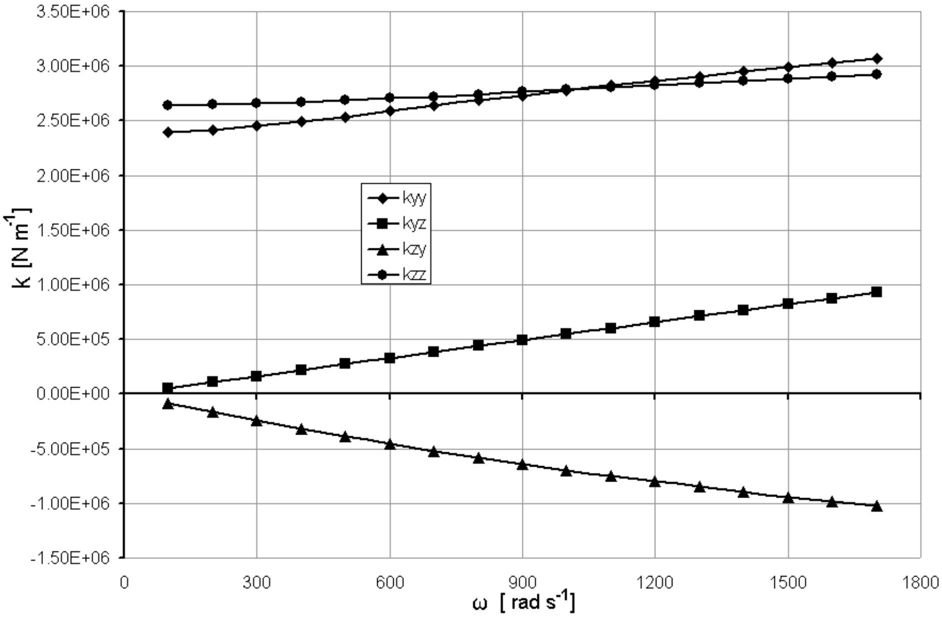

Figure 7: Stiffness vs. journal angular velocity ω, Bearing A

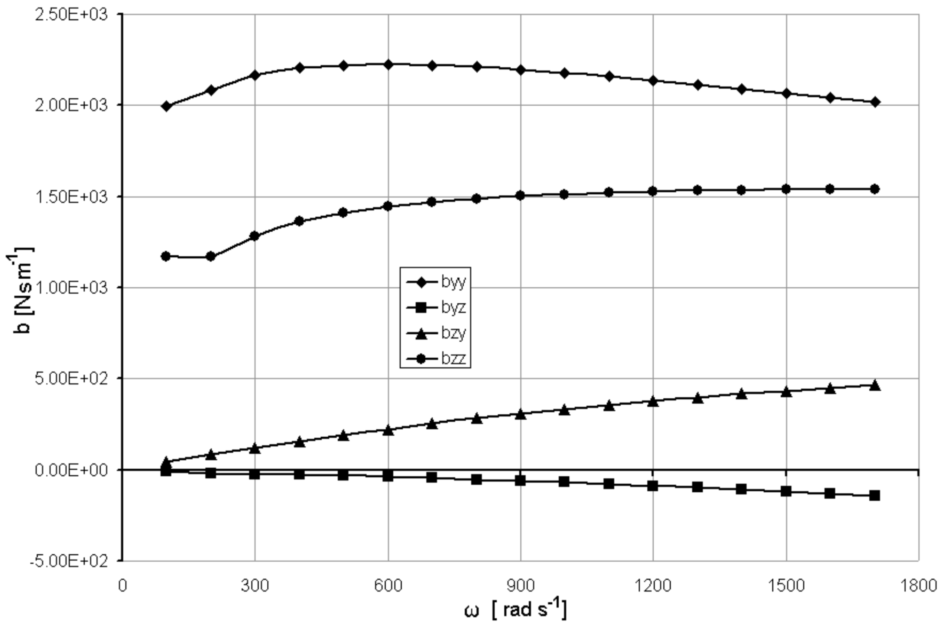

Figure 8: Damping coefficient vs. journal angular velocity ω, Bearing A

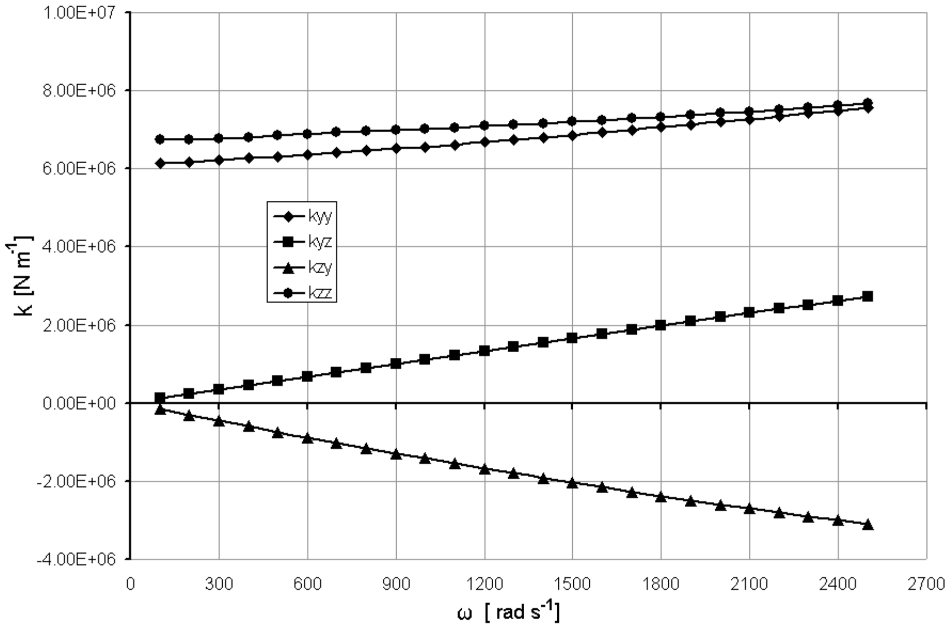

Figure 9: Stiffness vs. journal angular velocity ω, Bearing B

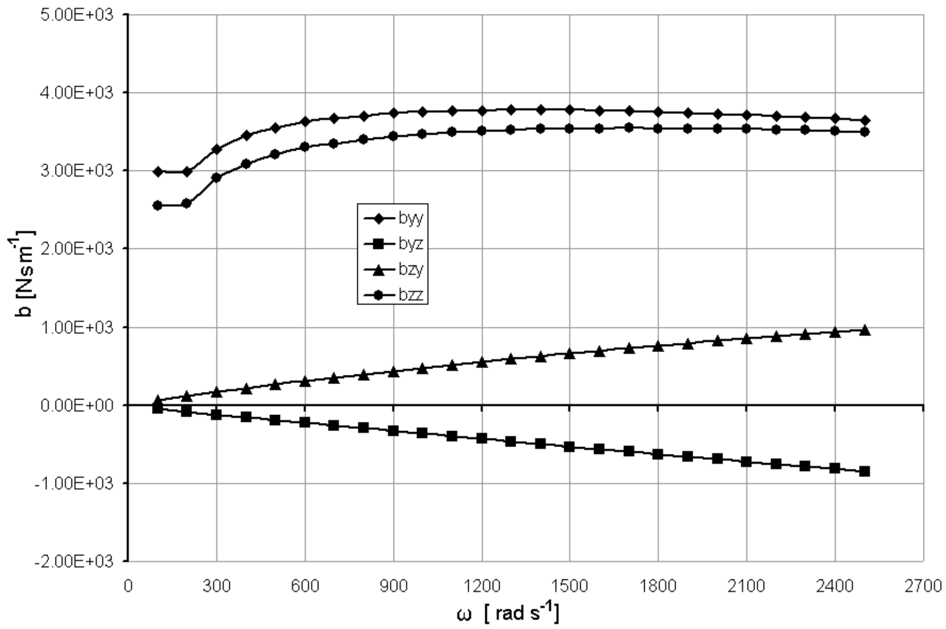

Figure 10: Damping coefficient vs. journal angular velocity ω, Bearing B

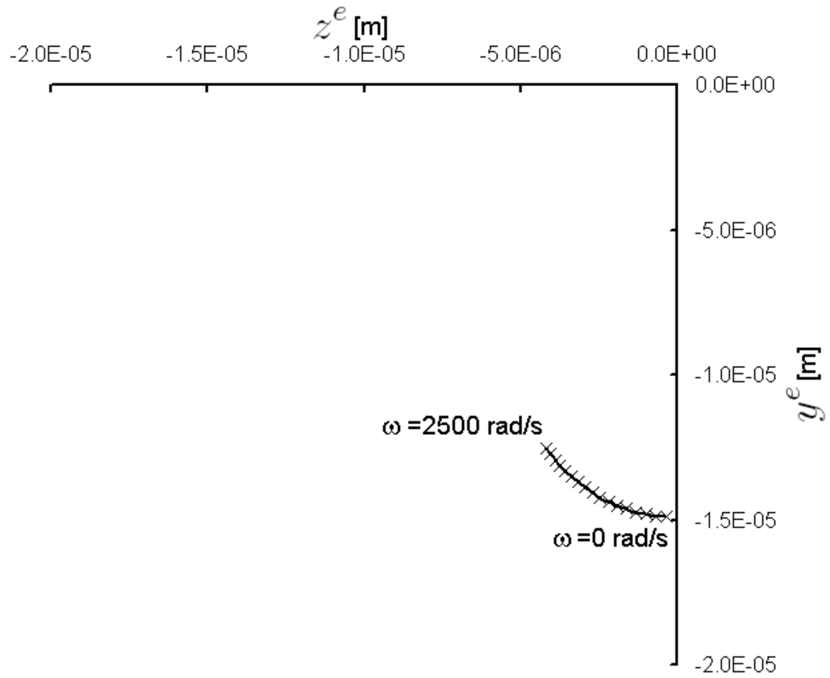

Figure 11: Equilibrium of journal centre, Bearing A

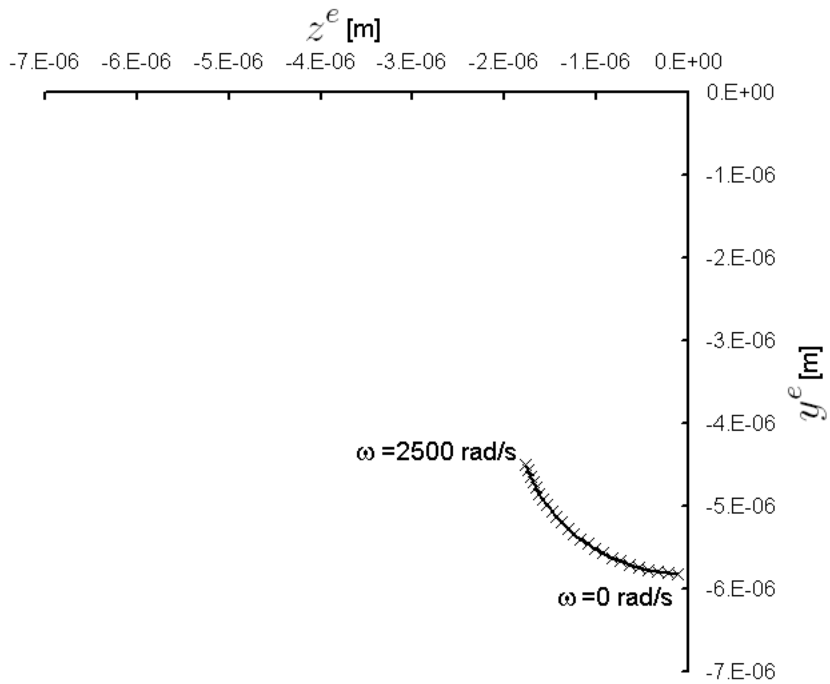

Figure 12: Equilibrium of journal centre, Bearing B

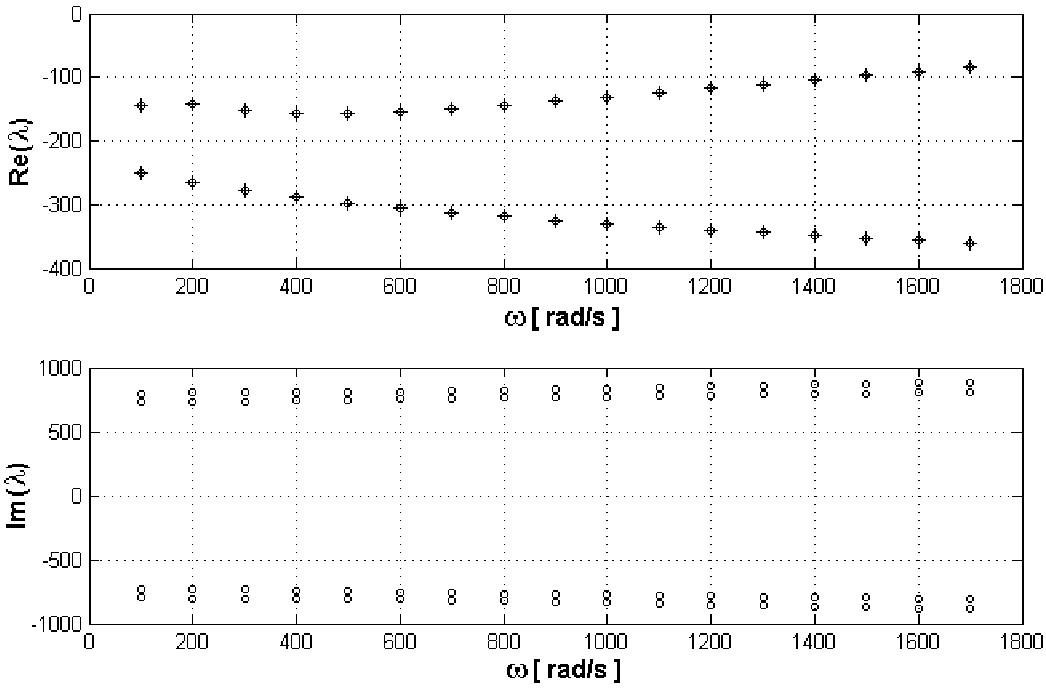

Figure 13: Eigenvalues vs. journal angular velocity ω, Bearing A

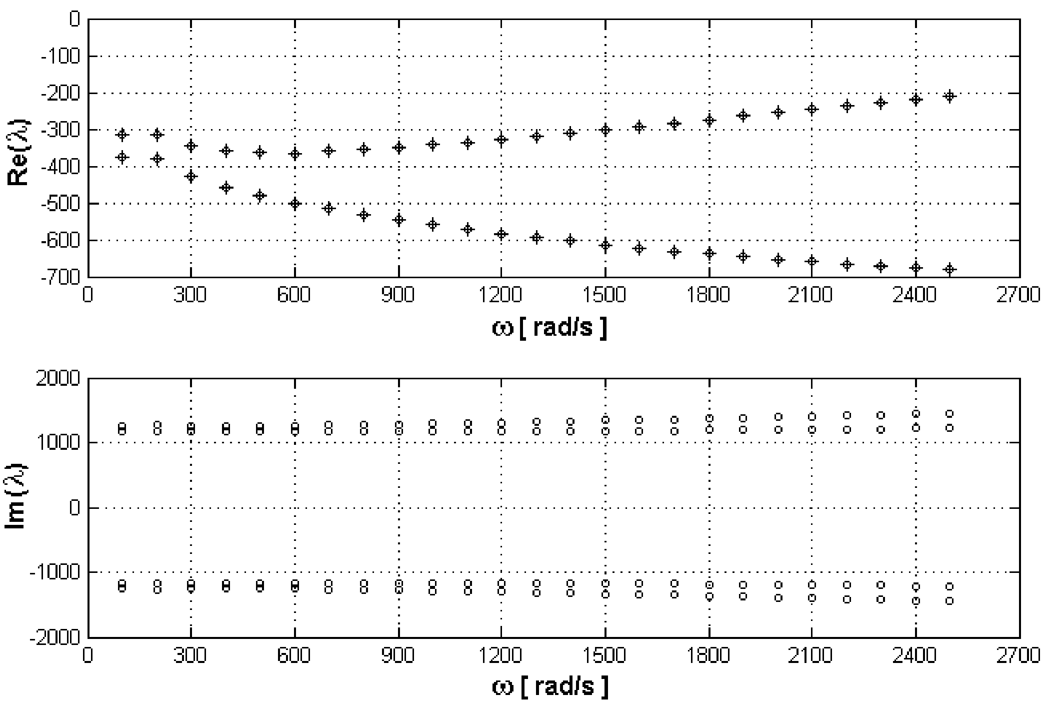

Figure 14: Eigenvalues vs. journal angular velocity ω, Bearing B

7. Conclusions

Linear stiffness and damping coefficients can be solved by presented method. Solutions of two examples of aerostatic bearings show relations between stiffness and damping coefficients and angular frequency of rotating journal. Obtained coefficients can be used for solving stability and amplitudes of steady-state vibrations by methods of linear algebra. Results of the method is to be verified by experiments.

8. Acknowledgement

This work was supported by the GA CR under project No. 101/06/1787 "Dynamic properties of gas bearings and their interaction with rotor".

9. References

Cioc, S., Dimofte, F., Keith, T. & Fleming, D. (2003) Computation of Pressurized Gas Bearings Using CE/SE Method. NASA/TM-2003-212110.

Czolczynski, K. (1994) Stability of High Stiffness Gas Journal Bearings. *Wear*, v. 172, p. 175-183.

Czolczynski, K. (1996) How to obtain stiffness and damping coefficients of gas bearings. *Wear*, v. 201, p. 265-275.

Czolczynski, K. & Kapitaniak, T. (1997) Hopf bifurcation in rotors supported in gas bearings. *Chaos, Solitons & Fractals*, v. 8, No.4, p. 499-515.

Czolczynski, K. (1999) *Rotordynamics of Gas-Lubricated Journal Bearing Systems.* Springer-Verlag New York Inc., New York.

Han, D.-Ch., Park, S.-S. & Kim J-W. (1994) A Study on the Characteristics of Externally Pressurized Air Bearings. *Precision engineering*, vol 16, no 3, p. 164-173.

Lo, Ch.-Y., Wang, Ch.-Ch., Lee & Y.-H. (2004) Performance Analysis of High-Speed Spindle Aerostatic Bearings. *Tribology International*, v. 38, p. 5-14.

Skarolek, A. & Kozánek, J. (2006) Matematický model radiálních aerostatických ložisek v interakci s rotorem. In: *Interaction and feedbacks '2006*, IT CAS, Prague.

Skarolek, A. (2007) Model of rotor supported in aerostatic journal bearings. In: *Applied Mechanics '2007*, Malenovice.

Šimek, J., Kozánek, J. & Steinbauer, P. (2007) Dynamic Properties of Aerostatic Journal Bearings. In: *Dynamics of Machines '2007*, IT CAS, Prague.